Unified integration of spatial transcriptomics across platforms

(SUPPLEMENTAL INFORMATION)

A Supplementary Note

Clustering performance of LLOKI-FP

To assess the quality of embeddings generated by LLOKI-FP, we compared them to embeddings produced by directly passing the gene expression matrix through scGPT, which serves as our baseline. We applied Leiden clustering to the embeddings generated by each method to produce clusters for metric evaluation. To ensure the number of clusters matched the ground truth, we performed an interval search to determine the resolution parameter that yielded the exact number of clusters as the ground truth. **Table** S1 shows the clustering performance using ARI and NMI scores. As shown, LLOKI-FP consistently outperforms the baseline across all datasets and metrics, demonstrating the effectiveness of our approach.

Hyperparameter choice for LLOKI-FP and LLOKI-CAE

Here we provide additional details on training LLOKI-FP and LLOKI-CAE, including hyperparameter selection and optimizations for training efficiency and performance.

For LLOKI-FP, we constructed k-NN graphs using $k = 40$ neighbors. As detailed in the **Methods** section, we employed the optimal transport stopping criterion to determine the number of feature propagation iterations. For the feature diffusion step, we empirically determined $\alpha = 0.05$ (self-weight = 0.95) as the optimal value for updating gene expression, and used only a single graph iteration.

LLOKI-CAE's loss function includes three distinct terms, each weighted by a corresponding parameter. The best results were obtained using $\lambda_{\text{rec}} = 1$, $\lambda_{\text{bc}} = 500$, and $\lambda_{\text{trip}} = 2$.

During early training, positive-anchor pairs selected for triplet loss may be suboptimal. To address this, we introduced a warm-up parameter w for the triplet weight. For the first w iterations, the triplet weight λ'_{trip} is scaled as follows:

$$\lambda'_{\text{trip}} := \min\left(\lambda_{\text{trip}}, \lambda_{\text{trip}} \times \frac{i - w + 1}{t}\right)$$

where t is the total number of training iterations and i is the current iteration. We used $w = 10$ for the warm-up parameter. Additionally, triplets were computed after each iteration to ensure continual improvement in the selection of possible triplets.

For the biological conservation loss, we use $k = 30$ neighbors, limited to cells from the same technology. This reduces the neighbor search space and reflects the observation that early in the training, meaningful neighbors are unlikely to come from other technologies.

For the triplet loss, mutual nearest neighbors (MNNs) between each pair of technologies were identified using $k = 40$. All MNNs were retained as anchor-positive pairs, and negative samples were drawn randomly from the same technology as the anchor. For the LLOKI run shown in **Fig.** 2, we utilized the optional cell type refinement described in the **Methods** section. Specifically, rather than using all MNNs, positive pairs were formed by randomly selecting cells from any batch that share the same cell type as the anchor. For negative sampling, instead of random selection, we chose the closest cell from the same batch that belonged to a different cell type. This hard negative sampling strategy improved embedding space differentiation by focusing on the most challenging cases for discrimination.

To manage GPU memory and enable frequent backpropagation, we implemented fixed mini-batching. Batches were computed once at the beginning of training and held constant throughout. This simplification reduces computational overhead and ensures that all neighborhood and triplet computations remain within-batch. We found that a batch size of 16,000 cells provided the best results.

Since the biological conservation loss and triplet loss functions operate on different numerical ranges, the values of λ_{bc} and λ_{trip} were selected to balance their contributions. For new datasets we recommend starting with the default values and, if needed, performing a coarse grid search over $\lambda_{\mathrm{trip}} \in \{1, 2, 4\}$ while keeping λ_{bc} fixed. To further enhance cell-type separability, λ_{bc} may be increased. This allows users to adjust the trade-off between biological conservation and batch mixing based on their analysis goals.

Creating a high-level cell type annotation

A key challenge when integrating ST datasets is the variation in available annotations. This variability complicates direct comparisons and the visualization of batch integration performance. To address this, we created a unified set of high-level cell type annotations for use in UMAP visualizations, while retaining the original annotations for evaluation using biological conservation metrics.

To generate this unified annotation, we aggregated the original cell type labels from four datasets (MERSCOPE, MERFISH, STARmap, and CosMx). We mapped these labels into eight broader categories that perserve key biological distinctions. These high-level annotations, along with the original cell types they encompass, are detailed in **Table** S3.

The Xenium dataset did not include cell type annotations but provided cluster identities. To annotate Xenium clusters, we used marker gene expression and spatial localization. Where marker genes were unavailable – for example, for astrocytes – we matched the spatial distribution of Xenium clusters to the known spatial patterns of annotated cell types in other datasets. This heuristic spatial mapping allowed us to assign high-level annotations even in the absence of canonical markers.

B Supplementary Tables

	scGPT		LLOKI-FP		LLOKI-FP – OT	
Dataset	**ARI**	**NMI**	**ARI**	**NMI**	**ARI**	**NMI**
MERSCOPE	0.541	0.740	0.727	0.830	0.606	0.793
MERFISH	0.605	0.795	0.892	0.893	0.893	0.903
STARmap	0.197	0.364	0.423	0.609	0.351	0.560
CosMx	0.347	0.555	0.395	0.599	0.370	0.607
Xenium	0.451	0.620	0.522	0.709	0.542	0.718

Table S1: Ablation study on cell-type clustering metrics (Adjusted Rand Index, ARI, and Normalized Mutual Information, NMI) comparing LLOKI-FP with scGPT and LLOKI-FP without the optimal transport alignment (*–OT*). Since optimal transport is a key component of LLOKI-FP, removing it enables us to evaluate its specific contribution to clustering performance. Results are shown for five spatial transcriptomics datasets: MERSCOPE, MERFISH, STARmap, CosMx, and Xenium. Higher ARI and NMI values indicate better clustering performance.

Dataset	ST sparsity	scRNA-seq sparsity
MERSCOPE	0.697	0.853
MERFISH	0.883	0.889
STARmap	0.907	0.875
CosMx	0.610	0.541
Xenium	0.678	0.792

Table S2: Sparsity comparison between five spatial transcriptomics datasets – MERSCOPE, MERFISH, STARmap, CosMx, and Xenium – and the scRNA-seq reference, subset to the gene panel for each ST dataset.

High-Level Annotation	**Corresponding Entries**
Astrocytes	Astrocytes_Cortex_Hippocampus, Astrocytes_Thalamus_Hypothalamus, Astrocytes, Astro-NT, Astro-TE, Astroependymal
Ependymal cells	Ependymal cells, Tanycytes, Choroid_plexus_epithelial_cells, Ependymal_cells, Tanycyte, Ependymal, CHOR
Excitatory neurons	CNU-HYa Glut, CNU-MGE GABA, Excitatory_neurons_Hippocampal_CA1, Excitatory_neurons_Hippocampal_CA2, Excitatory_neurons_Hippocampal_CA3, Excitatory_neurons_Layer1_Piriform, Excitatory_neurons_Layer2_3, Excitatory_neurons_Layer4, Excitatory_neurons_Layer5, Excitatory_neurons_Layer5_6, Excitatory_neurons_Layer6, Excitatory_neurons_Telencephalon, Peptidergic_neurons, Excitatory_neurons_Amygdala, Excitatory_neurons_Di/mesencephalon, Cholinergic_neurons_Habenebula, HY Glut, HY Gnrh1 Glut, HY MM Glut, IT-ET Glut, MB Glut, MH-LH Glut, MY Glut, NP-CT-L6b Glut, OB-CR Glut, P Glut, Telencephalon projecting excitatory neurons, Di- and mesencephalon excitatory neurons, TH Glut
Inhibitory neurons	Cck_interneurons, CNU-HYa GABA, CNU-LGE GABA, CNU-MGE GABA, CTX-CGE GABA, CTX-MGE GABA, Di- and mesencephalon inhibitory neurons, D1_medium_spiny_neurons, D2_medium_spiny_neurons, HY GABA, Inhibitory_interneurons, Inhibitory_neurons_Amygdala, Inhibitory_neurons_Habenula_Hypothalamus, Inhibitory_neurons_Habenula_Thalamus, Inhibitory_neurons_Reticular_nucleus, Interneurons, MB GABA, MY GABA, OB-IMN GABA, Olfactory inhibitory neurons, Peptidergic neurons, Serotonergic_neurons, Telencephalon_inhibitory_neurons, Telencephalon inhibitory interneurons, Telencephalon projecting inhibitory neurons
Microglia	Immune, Microglia
Oligodendrocytes	Commited_oligodendrocytes, Mature_oligodendrocytes, Oligodendrocyte precursor cells, Myelin_forming_oligodendrocytes, Newly_formed_oligodendrocytes, Oligodendrocytes, Oligodendrocytes_precursor_cells, OPC-Oligo
Other/Unannotated	Neuroblasts, Unannotated
Vascular cells	Choroid plexus epithelial cells, Vascular, Vascular and leptomeningeal cells, Vascular endothelial cells, Vascular_endothelial_cells, Vascular_leptomeningeal_cells, Vascular_smooth_muscle_cells, Vascular smooth muscle cells, Perivascular_macrophages, Pericytes

Table S3: Unified high-level cell type annotations derived, mapped from the four spatial transcriptomics technologies with available cell type annotations: MERFISH, MERSCOPE, STARmap, and CosMx.

Dataset	Strain	Sex	Age
MERFISH	C57BL/6NCrl (Charles River)	Female	56–62 weeks
MERSCOPE	C57BL/6J	Male	53–71 days
STARmap	C57BL/6 (Charles River)	Female	8–10 weeks
CosMx	C57BL/6J	Male	18 months
Xenium	C57BL/6	Unknown	Unknown

Table S4: Summary of mouse metadata for brain slices used across spatial transcriptomics technologies. To account for potential biological variability, we report the strain, sex, and age of mice used in each dataset, as specified by dataset sources.

C Supplementary Figures

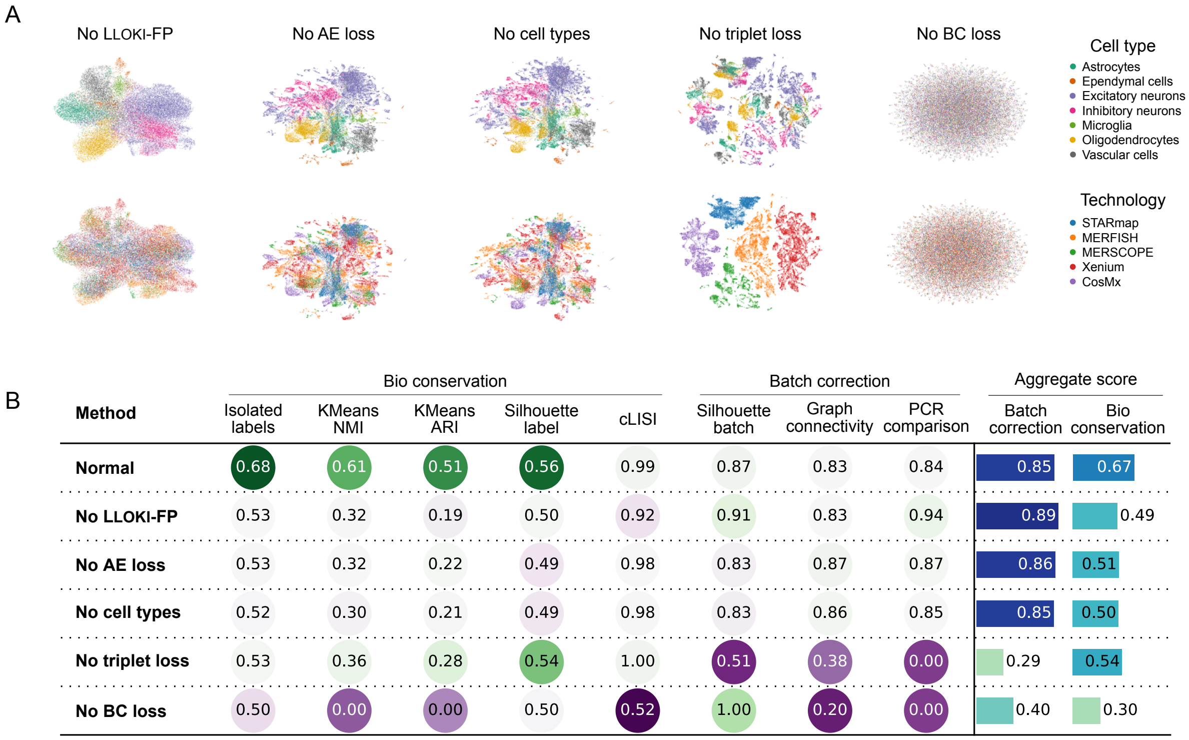

Method	Bio conservation					Batch correction			Aggregate score	
	Isolated labels	KMeans NMI	KMeans ARI	Silhouette label	cLISI	Silhouette batch	Graph connectivity	PCR comparison	Batch correction	Bio conservation
Normal	0.68	0.61	0.51	0.56	0.99	0.87	0.83	0.84	0.85	0.67
No LLOKI-FP	0.53	0.32	0.19	0.50	0.92	0.91	0.83	0.94	0.89	0.49
No AE loss	0.53	0.32	0.22	0.49	0.98	0.83	0.87	0.87	0.86	0.51
No cell types	0.52	0.30	0.21	0.49	0.98	0.83	0.86	0.85	0.85	0.50
No triplet loss	0.53	0.36	0.28	0.54	1.00	0.51	0.38	0.00	0.29	0.54
No BC loss	0.50	0.00	0.00	0.50	0.52	1.00	0.20	0.00	0.40	0.30

Figure S1: Ablation study of LLOKI performance when removing components of the three part loss function of LLOKI-CAE or LLOKI-FP. **(A)** UMAP visualizations for each ablation, with cells colored by cell type (top) and by technology (bottom). Variants include LLOKI-CAE with the biological conservation loss, triplet loss, or reconstruction loss removed. One variant additionally uses cell-type based sampling to define positive pairs for triplet loss. LLOKI-FP is also ablated by directly passing raw gene expression through scGPT without LLOKI-FP. **(B)** Performance comparison of the five ablations using eight metrics, assessing biological variation preservation and batch mixing across technologies.

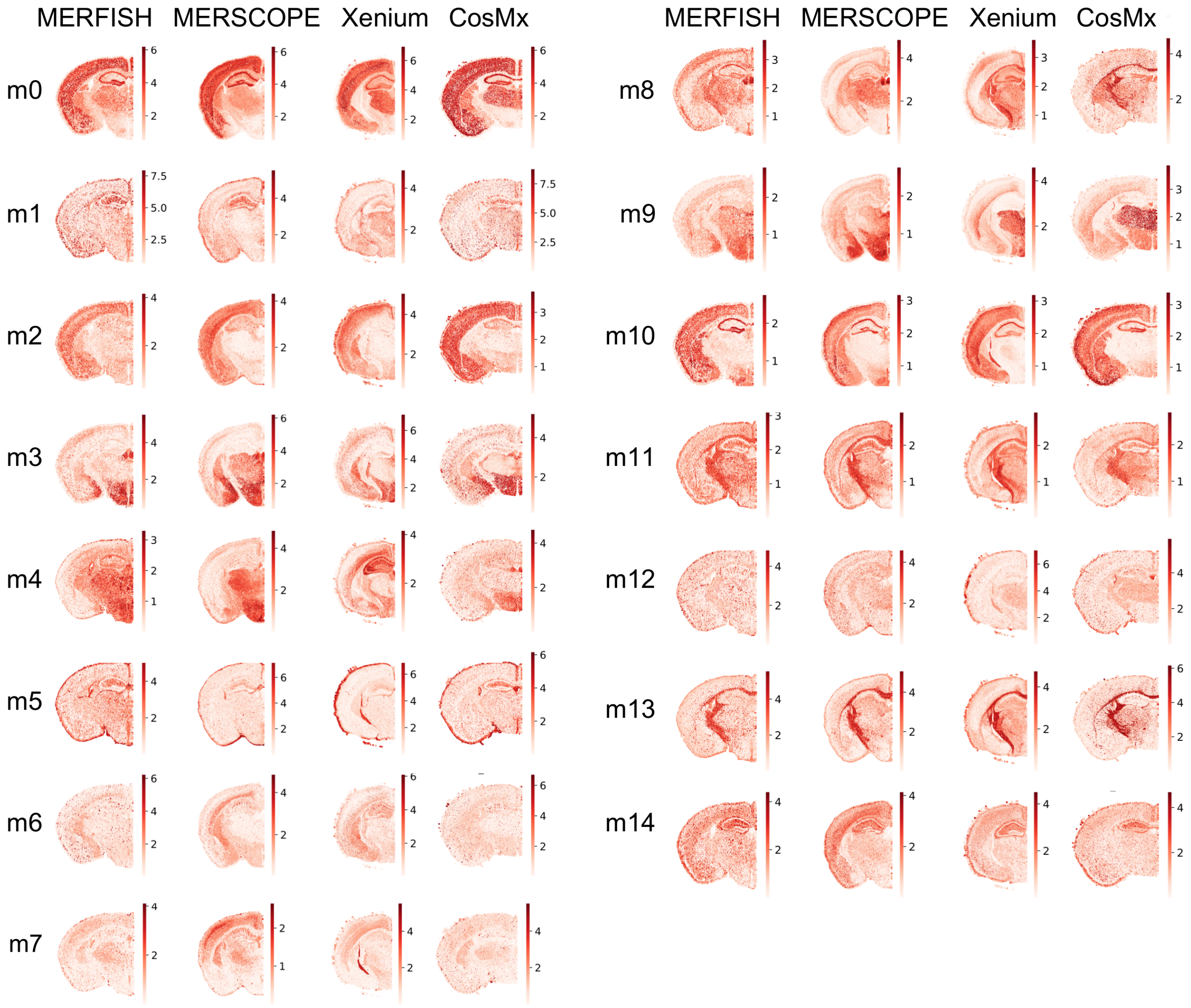

Figure S2: *In situ* expression patterns of the 15 metagenes identified by SpiceMix+ Lloki across four spatial transcriptomics technologies: MERFISH, MERSCOPE, Xenium, and CosMx. Each row corresponds to one of the 15 metagenes (m0-m14), and each column displays its spatial expression pattern within a given technology. Darker colors indicate higher expression levels.

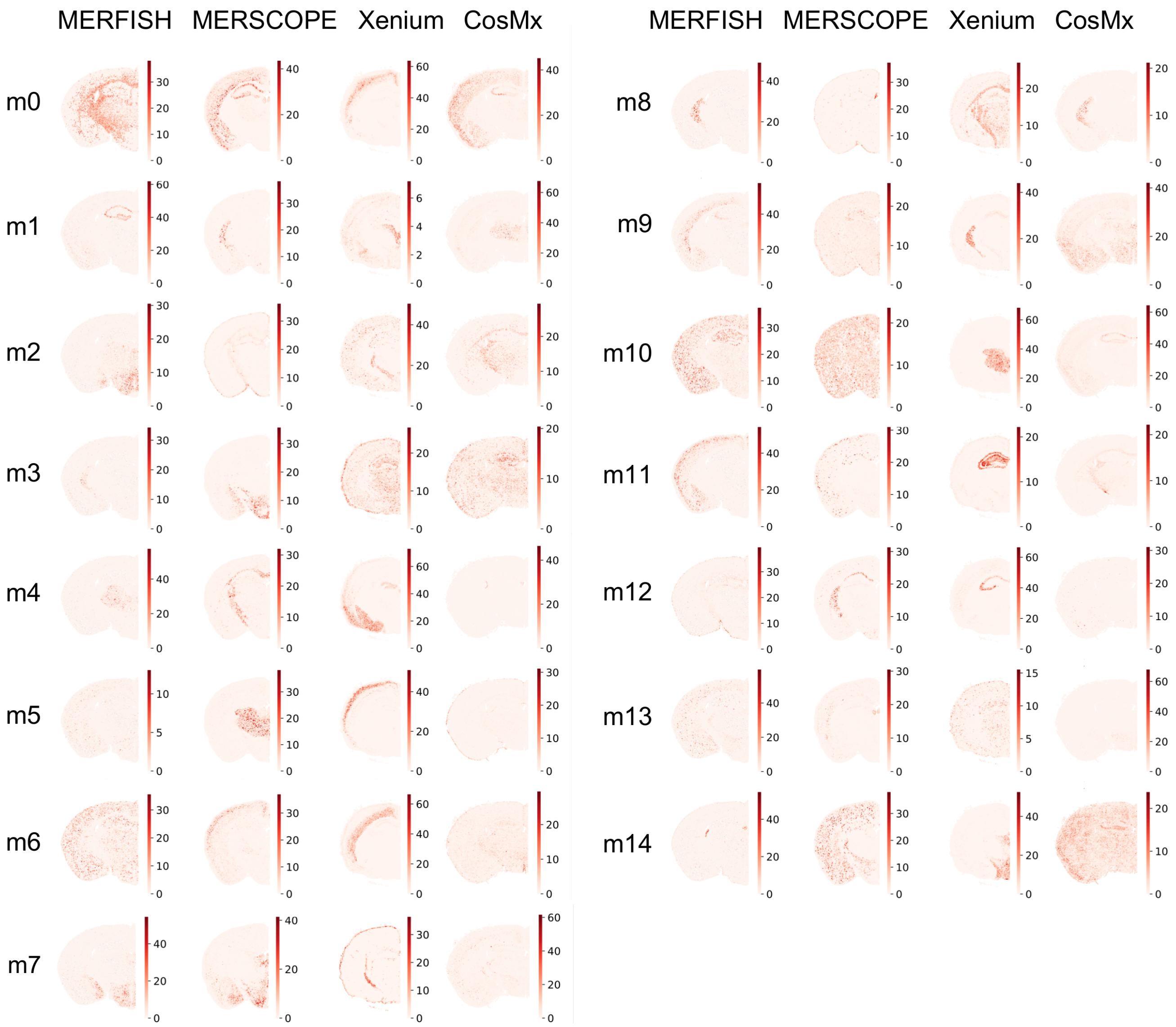

Figure S3: *In situ* expression patterns of the 15 metagenes identified by SpiceMix on the shared gene set (22 genes) across four spatial transcriptomics technologies: MERFISH, MERSCOPE, Xenium, and CosMx. Each row corresponds to one of the 15 metagenes (m0-m14), and each column displays its spatial expression pattern within a given technology. Darker colors indicate higher expression levels.

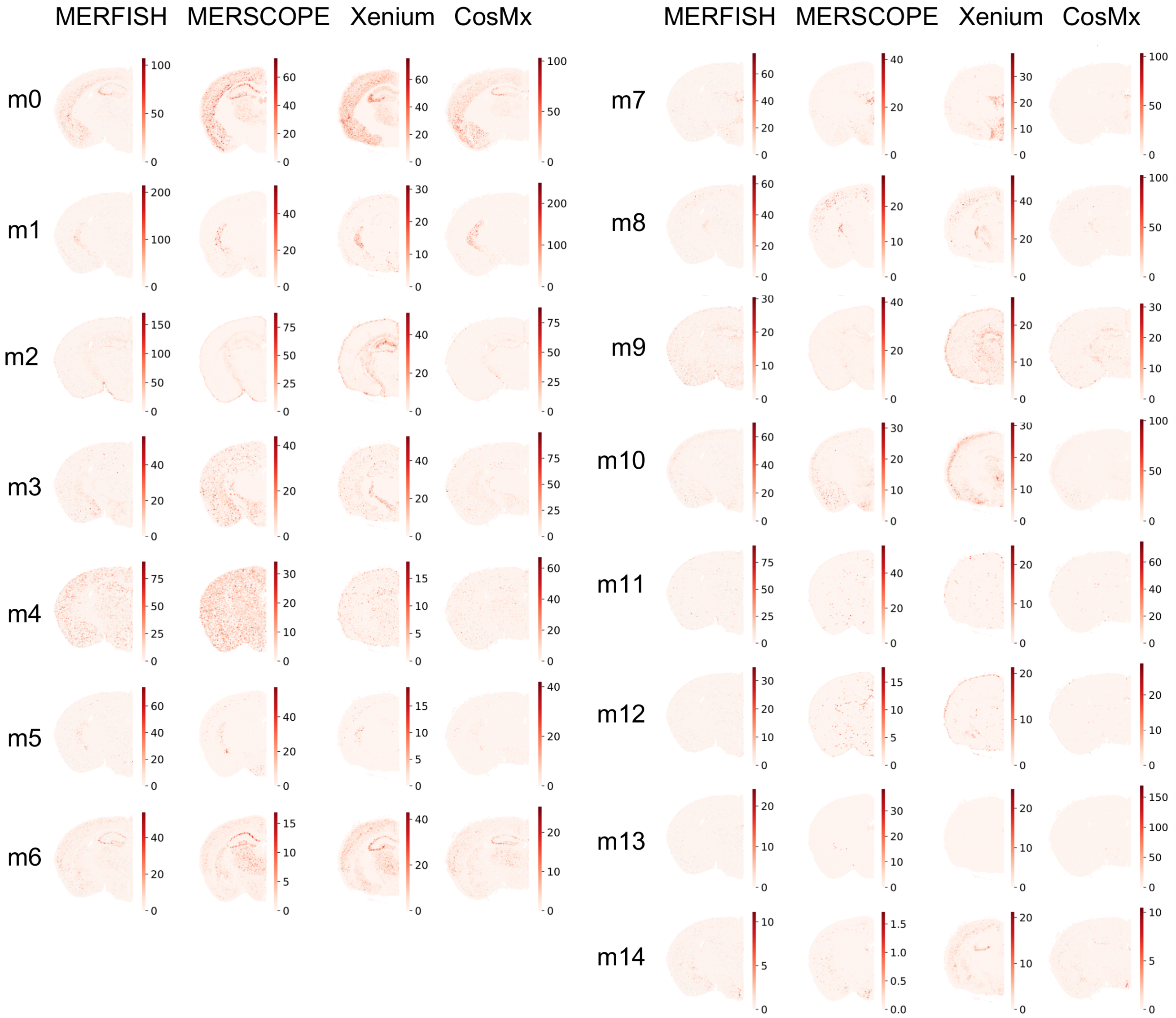

Figure S4: *In situ* expression patterns of the 15 metagenes identified by independent SpiceMix runs performed separately on each spatial transcriptomics technology: MERFISH, MERSCOPE, Xenium, and CosMx. Each row corresponds to one of the 15 metagenes (m0–m14), and each column displays its spatial expression pattern of that metagene in the respective technology. Darker colors indicate higher expression levels.

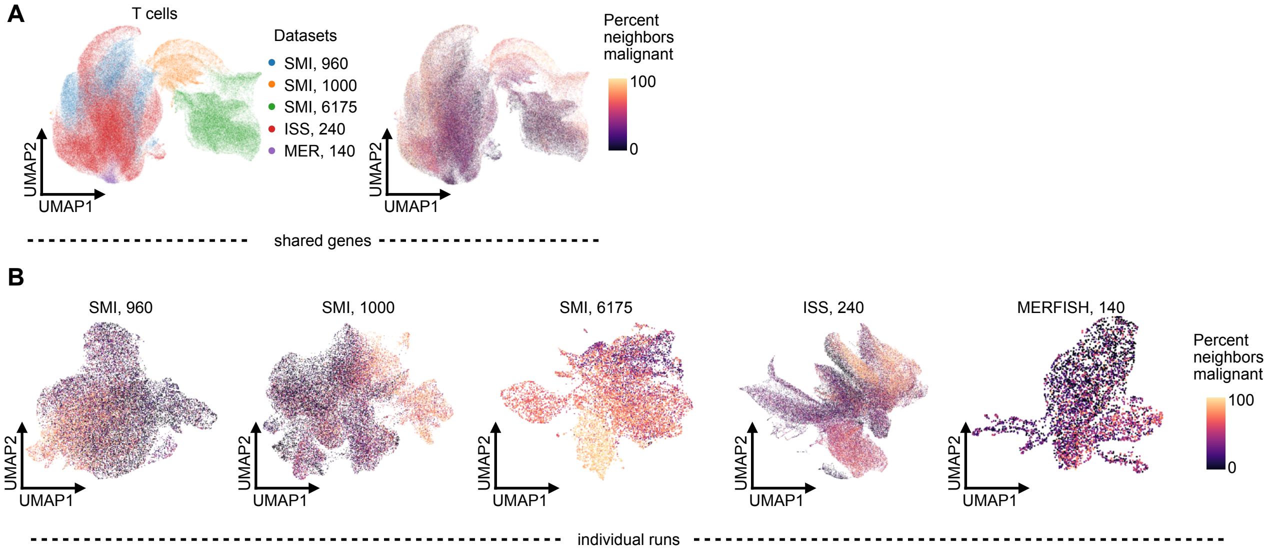

Figure S5: UMAP visualization of T cells using shared genes and individual dataset runs. **(A)** UMAP of T cells using the shared gene set across all five datasets, colored by dataset (left) or by the proportion of the 100 nearest spatial neighbors that are malignant (right). **(B)** UMAP of T cells using the full gene panel measured for each dataset individually, colored by the proportion of the 100 nearest spatial neighbors that are malignant.